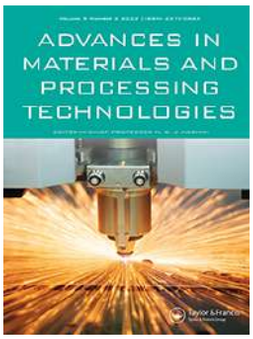

Advances in Materials and Processing Technologies

ISSN: (Print) (Online) Journal homepage: https://www.tandfonline.com/loi/tmpt20

Modeling and analysis of multi-functional self-healing material using Runge-Kutta Method for investigation of aircraft wing structure

Usha Pawar, Shivaji G. Chavan, Kiran Suresh Bhole, Mansing Rathod, Dipali Bhole, Ankit D. Oza, Manoj Kumar, Manish Gupta, Satbir S. Sehgal & Manoj Kumar

To cite this article: Usha Pawar, Shivaji G. Chavan, Kiran Suresh Bhole, Mansing Rathod, Dipali Bhole, Ankit D. Oza, Manoj Kumar, Manish Gupta, Satbir S. Sehgal & Manoj Kumar (09 Oct 2023): Modeling and analysis of multi-functional self-healing material using Runge-Kutta Method for investigation of aircraft wing structure, Advances in Materials and Processing Technologies, DOI: 10.1080/2374068X.2023.2264577

To link to this article: https://doi.org/10.1080/2374068X.2023.2264577

Published online: 09 Oct 2023.

ADVANCES IN MATERIALS AND PROCESSING TECHNOLOGIES
https://doi.org/10.1080/2374068X.2023.2264577

Modeling and analysis of multi-functional self-healing material using Runge-Kutta Method for investigation of aircraft wing structure

Usha Pawar[a], Shivaji G. Chavan[a], Kiran Suresh Bhole[b], Mansing Rathod[c], Dipali Bhole[d], Ankit D. Oza[e], Manoj Kumar[f], Manish Gupta[g], Satbir S. Sehgal[h] and Manoj Kumar[i]

[a]Department of Mechanical Engineering, Datta Meghe College of Engineering, Navi Mumbai, India; [b]Department of Mechanical Engineering, Sardar Patel College of Engineering, Mumbai, India; [c]Department of Information Technology, KJ Somaiya Institute of Engineering and Information Technology, Mumbai, India; [d]Department of Computer Engineering, Shree L. R. Tiwari College of Engineering, Mumbai, India; [e]Department of Mechanical Engineering, Parul University, Vadodara, Gujarat, India; [f]Department of Mechanical Engineering, Chandigarh University, Gharuan, Punjab, India; [g]Division of Research & Development, Lovely Professional University, Phagwara, Punjab, India; [h]Division of Research & Innovation, Uttaranchal University, Dehradun, Uttarakhand, India; [i]Department of Mechanical Engineering, ABES Engineering College, Ghaziabad, India

ABSTRACT

This paper presents the deployment of Runge-Kutta method to overcome the main challenge in analysis of failure of aircraft wing structure subjected to wind pressure and point loading. Failure phenomenon of any structure is time dependents and is typically referred as dynamic in engineering mechanics and is fairly a complex to investigate. In this context, the dynamic analysis concept has successfully implemented by using computer program in SCILAB software. The numerical technique is adopted as Runge-Kutta fourth order (RK4) method for performing dynamic behaviour of wind structure. The demonstration of failure mode of wing structure is based on function of time. The numerical approach is deemed to provide a detailed description of these phenomena affecting the overall dynamic of failure envelope of wing structure. The parametric study is presented; likewise the effect on failure of wing structure by changing different wind pressure, length and moment, respectively. The wing structure is analytically validated against available literature. Finally, others important failure results obtained from this analysis has discussed in detail.

ARTICLE HISTORY
Accepted 22 September 2023

KEYWORDS
FEM; dynamic failure criteria; Runge-Kutta fourth order (RK4) computational method; ANSYS

1. Introduction

Most of theoretical failure mode investigation and its practical dynamic failure response have been addressed by several studies, typically for aircraft wing structure [1–10]. Study [1] has investigated the new solution for damage of composite beam. Similarity solution and RK method is widely used for analysis of a thermal boundary layer model at the entrance region of a circular tube [2]. The study of advance Spectral analysis and

CONTACT Ankit D. Oza ankitoza6060@yahoo.in Department of Mechanical Engineering, Parul University, Vadodara, Gujarat 391760, India

modelling of the spray liquid injection in a Lean Direct Injection (LDI) gas turbine combustor through Eulerian-Lagrangian Large Eddy was simulated in [3]. Study [4] focused on the effects of loading rate and heterogeneity of meso-/micro-structure on the failure pattern and the macroscopic mechanical properties of concrete. The experimental methods of dynamic photo elasticity, optical caustics and the numerical method of finite element technique are utilised in [5]. Research on seismic dynamic response characteristics of weak surrounding rock slope with double-arch tunnel is explored in [6]. The aerodynamic performance and flight stability characteristics significantly affected by multiple-propeller operation, aerodynamic analysis reflecting the power-on effect required for design [7]. Study [8] presented a new technique consists of explicit fourth-order Runge-Kutta (RK4) method for the dynamic system. The method discretized system by the explicit RK4 method under the assumption of linear interpolation for the dynamic load, leading to a recurrence equation for the current state. A Newton iteration-based interval analysis method for nonlinear structural systems with uncertain-but-bounded parameters is studied in [9]. Study [10] demonstrated simplified numerical method for nonlocal static and dynamic analysis of a graphene nanoplate. Research [11] presented analysis of the strain energy release rate for time-dependent delimitation in multilayered beams with creep. As a case study, the analytical solutions are then checked against numerical solution programming by FORTRAN code obtained via using Runge-Kutta fourth order (RK4) method [12]. Researchers [13] determine the dynamic response and failure mode of sandy slope subjected simultaneously to seismic forces and variable groundwater conditions. However, such systems of computational method are developed to study the dynamics of lightweight deployable structures without damping. Theory and implementation strategy of the developed method is presented in [14]. Numerical analysis for deformation and failure characteristics of deep roadway surrounding rock under static-dynamic coupling stress is analysed in [15]. Numerical analysis of evaluation methods and influencing factors for dynamic stability of bedding rock slope were investigated in [16]. The study of failure dynamic response law is the foundation of slope dynamic stability analysis, including responses of acceleration, velocity, displacement, and stress-strain equivalents [17]. Study [18] presented coupled steel plate shear wall (C-SPSW), one of the resisting systems with high ductility and energy absorption. Energy dissipation in the C-SPSW system is accomplished by the bending and shears behaviour of the link beams and SPSW. Study [19] developed differential quadrature method (DQM) for forced vibrations and resonance frequency analysis of functionally graded (FG) nano-size beams rested on elastic substrate. The investigation has been studied utilising a shear deformation refined beam theory which contains shear deformations influence needless of any correction coefficient. Study [20] analysed the ballistic impact of WC-8Co on ceramic targets. The analytical results were verified by experiment and Numerical approaches [21]. The multiple states mechanical design problems and a systematic prescriptive process for supporting synthesis of a larger solution space were studied [21]. They also further set a modification rules and a database of building blocks has been developed. This has further supported the synthesis process.The fracture toughness was determined for critical Stress-Strain and energy release rate model using unconventional test method referred to as Spherical Indentation test to reduce the large and costly experimental set up as required in conventional fracture toughness Test [22, 23]. The presence of a crack significantly reduces the load bearing capacity of a structure

made of fracture prone material. The conventional process of repairing a defect is gouging and filling the gouged location by welding. In an attempt to overcome the limitation of the conventional repair process, repairing a defect using composite patch is proposed. The crack-tip radius effect on fatigue crack growth (FCG) of a mode I crack and near-tip stress-strain fields in such plastically compressible solids was investigated in [24]. Study also discussed plastically compressible materials characterised by elastic-viscoelastic constitutive equations. Study [25] has presented machine learning (ML) deployment for chemists and materials scientists who have no prior familiarity with these approaches. The Forming Limit Diagram, a crucial tool in metal forming operations that shows the failure limits for ductile damage and on-site necking, was examined in [26]. Research [27] presented, adding novel chemicals and ingredients to conventional lime mortars that may engineer their ability to self-heal, or be capable of mending a mechanical harm that has already happened. Both microscopic and macroscopic levels of the phenomenon of self-healing are possible, and in some cases, it can be started by a dispersed phase that becomes available as a result of mechanical injury. The flexible strain sensor developed in [28,29] is made of a multifunctional, self-healing, self-adhesive, and conductive sodium alginate/poly(vinyl alcohol) composite hydrogel.The aim of this paper is to present an analytical solution to failure dynamic analysis of aircraft wing structure subjected to wind pressure. RK4 computational technique is utilised to carry out the dynamic response.Predicting performance of aircraft wing structure when exposed to uniform wind pressure is the major goal in the study. Additionally, the impact of geometrical size and loading on structural failure is also examined.Several steps have been discussed here on the governing equation of the dynamic equation to reach the solution.The available literature in the field of dynamic response of structure is then used to validate the results. The computer code in SCILAB is developed for dynamic failure wing structure by adopting Runge-Kutta fourth order algorithm. A relatively small amount of researchers have focused on investigating airplane structure failure due to dynamic reaction. An analytical solution to the failure dynamic analysis of an aircraft wing structure subjected to wind pressure is the objective of this work. (Wang and Sun, 14) only examined the deformation of structures that were continuously loaded. However, the Runge-kutta method is currently being used to simulate mathematically complex self-healing materials in order to examine aircraft wing designs. RK4 computational technique is used to perform the dynamic response. Predicting the dynamic failure response of a multi-functional self-healing material for an aviation wing structure exposed to uniform wind pressure, etc., is our main goal. Additionally, the impact of geometrical dimension and loading on aircraft wing structure failure was explored. On the governing equation of the dynamic equation, several steps to the solution have been covered here. We next verified findings from some published research in the area of structural dynamic response. By using the Runge-Kutta fourth order algorithm, SCILAB's computer code for dynamic failure wing structures was created.

2. Central theme on the analytical scheme

The aircraft wing structure mostly fails due to wind and moment of wing. The static and dynamic modes of failures are mainly studied to get complete solution of problem. This time dependent loading condition in dynamic analysis for aircraft wing structure is

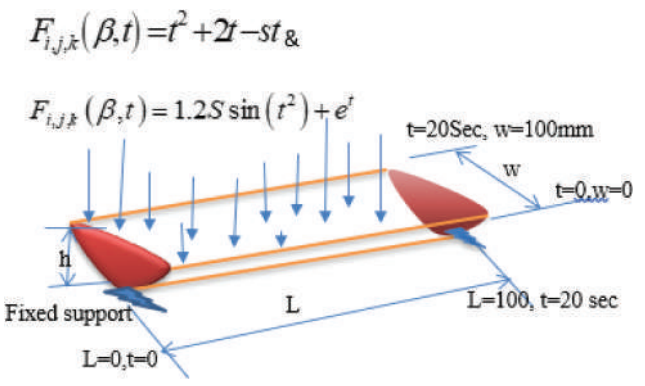

Figure 1. Aircraft wing structure free body diagram and boundary condition.

shown in Figure 1. The RK4 order computational approach is used to find dynamic response. Many of researcher have addressed the same problem; but this study emphasise and explore the research gap in the field on dynamic failure response of wing structure.

3. Numerical modeling and analysis

Finite element analysis for aircraft structure subjected to uniform wind pressure and thermo mechanical loading is considered in this study. The governing model for static analysis is given by Equation 1 and Equation 2

$$\{F_{ij}\} = [C_{ijkl}]\{U\} \tag{1}$$

$$\{U\} = \{F_{ij}\}[C_{ijkl}]^{-1} \tag{2}$$

Where, $\{F_{ij}\}$is force vector for overall structure, $[C_{ijkl}]$= Assembly (global) stiffness Matrix $\{U\}$=nodal deformation vector. The Equation 2 is solved by using ANSYS solver, to get deformation of all nodes. Further Equation 3 and Equation 4 is used to determine strain in direction (x,y,z)

$$\varepsilon_{ij} = \frac{\partial\{U\}_{x,y,z}}{\partial x, y, z} \tag{3}$$

Stress can be defined as

$$\sigma_{ij} = E\{\varepsilon_{ij}\} \tag{4}$$

The static analysis is carried out by using ANSYS software. Aerospace wing structure is discretized into SOLID 45 element with 2548 elements for present analysis. Two type of loading viz; point and wind pressure is considered in the analysis. Point load is simulated in Figure 2(a,b) while results of analysis on aircraft wing structure subjected to wind pressure are depicted in Figure 2(c,d).

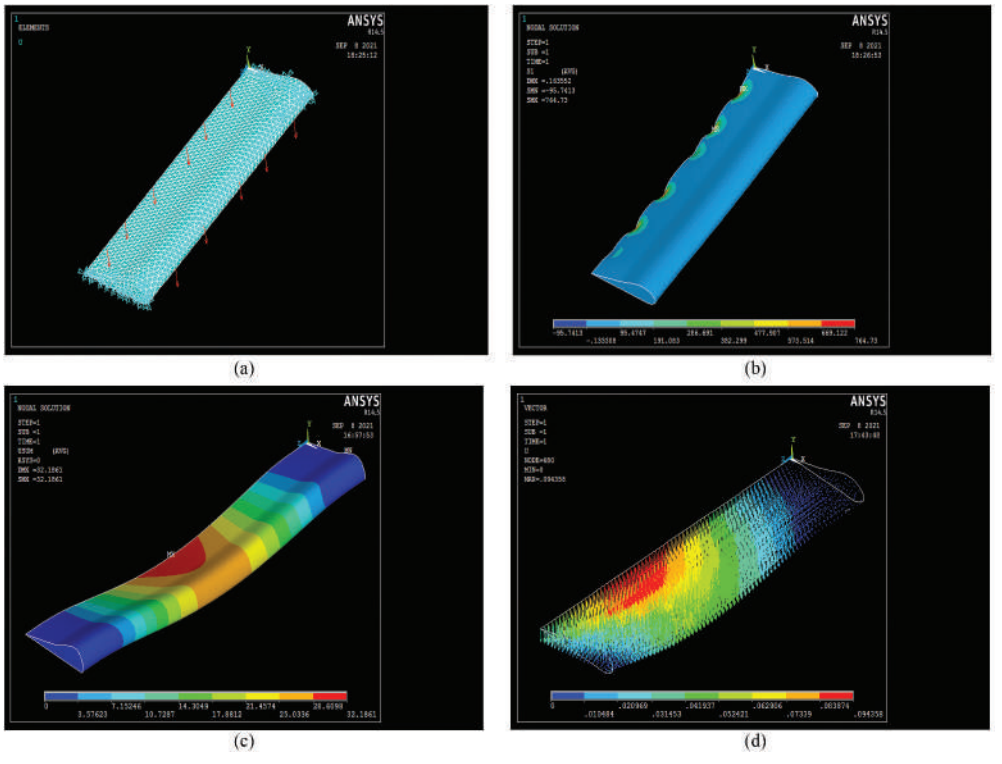

Figure 2. ANSYS simulation of results for aircraft wing structure, (a) point loading of wing structure model given boundary condition, (b) point loading displacement simulation of wing structure,(c)The simulation aircraft wing structure is subjected to wind pressure d) wing structure with wind pressure.

4. Mathematical modelling of self-healing material for aircraft wing structure

The impacts of damage on remaining stiffness and strength serve as a metaphor for damage in this section. There is no attempt to pinpoint the precise micro structural damage modes. However, some model elements, such as the damage variable used with few oversimplifying assumptions. The damage variable and the damage evolution equations are the three essential components of the model. Microcapsules made of urea-formaldehyde and dicyclopentadiene (DCPD) are used in the modelling. In the course of hand layup, the healing substance DCPD is first encapsulated and then dispersed in epoxy resin.In a similar way, the catalyst is also enclosed and distributed. The samples are consolidated using the vacuum bagging process once they have cured at room temperature. Distributed stiffness and strength losses result in aero plane wing structure failure. The amount of material parameters needed to describe the phenomenon and the precision of model projections are directly impacted by the damage variable selection. The integrity tensor (refer Equation 5 is defined as,

$$\psi = \sqrt{I - D} \tag{5}$$

where, I and D is second order identity and damage tensor, respectively;

The transformation of stress and strain between effective and damaged configurations is proficient by equation (6)

$$\vec{\sigma}_{ij} = \widehat{M}_{ijkl}\sigma_{kl} \; and \; {}^{-}\varepsilon_{ij} = M_{ijkl}\varepsilon^{hs}_{kl} \tag{6}$$

Where,ε^{hs}_{kl} is the strain for self-healing material, strain for aircraft wing structure, subjected to uniform wind pressure, M is the damage effect tensor defined as given in Equation 32:

$$M_{ijkl} = \frac{1}{2}\left(\psi_{ik}\psi_{jl} + \psi_{il}\psi_{jk}\right) \tag{7}$$

The stress–strain relationship for DCPD material is simply a linearly elastic material with model given in equation (8).

$$\vec{\sigma}_{ij} = \bar{C}_{ijkl}\varepsilon^{hs}_{kl}; \varepsilon^{hs}_{kl} = \bar{C}^{-1}{}_{ijkl}\sigma_{kl} = \vec{S}_{ijkl}\vec{\sigma}_{kl} \tag{8}$$

The constitutive equations in the failure self-healing material for aircraft wing structure are obtained by substituting Equations 8 into Equations 6, to receive equations (9-11):

$$\sigma_{ij} = \widehat{M}_{ijkl}\vec{\sigma}_{kl} = \widehat{M}_{ijkl}\bar{C}_{ijkl}\varepsilon^{hs}_{kl}\varepsilon^{e}_{ij} = M^{-1}_{ijkl}\varepsilon^{hs}_{kl} = M^{-1}_{ijkl}\bar{S}_{ijkl}\bar{\sigma}_{rs} \tag{9}$$

$$\sigma_{ij} = \widehat{M}_{ijkl}\vec{\sigma}_{kl} = \widehat{M}_{ijkl}\bar{C}_{ijkl}\varepsilon^{hs}_{kl}\varepsilon^{e}_{ij} = M^{-1}_{ijkl}\bar{S}_{krls}\bar{\sigma}_{tu} \tag{10}$$

$$\sigma_{ij} = \bar{C}_{ijkl}\varepsilon^{e}_{kl}\varepsilon^{e}_{ij} = \bar{S}_{ijkl}\bar{\sigma}_{kl} \tag{11}$$

Where, Cand S is stiffness and damage tensor for self-healing material, respectively.The potential energy for thermodynamic approach for thermoelastic analysis: The constitutive equations are derived from thermodynamic principles. The Helmholtz free energy includes the elastic energy and additional terms to represent the evolution of the internal parameters are presented in Equation 32-Equation 32:

$$\lambda = \boldsymbol{\phi}(\varepsilon, \varepsilon^{p}, D) - C^{d}_{1}\left[C^{d}_{2}e^{\left(\frac{\delta}{C^{d}_{2}}\right)}\right] - C^{p}_{1}\left[C^{p}_{2}e^{\left(\frac{\delta}{C^{p}_{2}}\right)}\right] \tag{12}$$

Where,ε and ε^{p} are elastic and plastic strain for self-healing material, p and δ is hardening variable. $C^{d}_{1}, C^{d}_{2}, C^{p}_{1}, C^{p}_{2}$are the material parameter for present model.

The equations (17–19) depicting thermodynamic state laws can be obtained by satisfying the Clausius-Duhem inequality, thus assuring non-negative dissipation:

$$\sigma_{ij} = \frac{\partial\lambda}{\partial\varepsilon^{e}_{ij}} = C_{ijkl}\left(\varepsilon_{kl} - \varepsilon^{p}_{kl}\right) = C_{ijkl}\varepsilon^{e}_{kl} \tag{13}$$

$$F_{ij} = -\frac{\partial\lambda}{\partial D_{ij}} = -\frac{1}{2}\left(\left(\varepsilon_{kl} - \varepsilon^{p}_{kl}\right)\right)\frac{\partial C_{klpq}}{\partial D_{ij}}\left(\varepsilon_{pq} - \varepsilon^{p}_{pq}\right) = -\frac{1}{2}\varepsilon^{e}_{ij}\frac{\partial C_{klpq}}{\partial D_{ij}}\varepsilon^{e}_{pq} \tag{14}$$

$$\mu(\delta) = --\frac{\partial\lambda}{\partial\delta} = C_1^d\left[e^{\left(\frac{\delta}{C_2^d}\right)} - 1\right] \tag{15}$$

$$\chi(p) = --\frac{\partial\lambda}{\partial p} = C_1^p\left[e^{\left(\frac{\delta}{C_2^d}\right)} - 1\right] \tag{16}$$

Where, $\sigma_{ij}, F_{ij}, \mu, \chi$are the thermodynamic force associates with internal variable$\delta, \varepsilon, p, D$.

The thermodynamic forces can be written in terms of stress (refer Equation 32-Equation 32,

$$F_x(t,T) = \frac{1}{\psi_x^2}\left(\frac{\vec{S}_x}{\psi_x^4}\sigma_x + \frac{\vec{S}_{xy}}{\psi_x^2\psi_y^2}\sigma_y\sigma_x + \frac{\vec{S}_{xy}}{\psi_x^2\psi_z^2}\sigma_y\sigma_z + \frac{2\vec{S}_{xy}}{\psi_x^2\psi_z^2}\sigma^2{}_x\right) \tag{17}$$

$$F_y(t,T) = \frac{1}{\psi_y^2}\left(\frac{\vec{S}_y}{\psi_y^4}\sigma_y + \frac{\vec{S}_{yz}}{\psi_y^2\psi_z^2}\sigma_y\sigma_z + \frac{\vec{S}_{zy}}{\psi_y^2\psi_z^2}\sigma_y\sigma_x + \frac{2\vec{S}_{zy}}{\psi_y^2\psi_z^2}\sigma^2{}_y\right) \tag{18}$$

$$F_z(t,T) = \frac{1}{\psi_z^2}\left(\frac{\vec{S}_z}{\psi_z^4}\sigma_z + \frac{\vec{S}_{zx}}{\psi_z^2\psi_x^2}\sigma_x\sigma_z + \frac{\vec{S}_{zx}}{\psi_z^2\psi_x^2}\sigma_x\sigma_z + \frac{2\vec{S}_{zx}}{\psi_x^2\psi_z^2}\sigma^2{}_z\right) \tag{19}$$

Present mathematical model is developed by considering wind force and systems (wing structure) in the same direction. The applied force magnitude is large while wind force and systems (wing structure) is in opposite direction. The failure criteria for self-healing material are given by Equation 32,

$$\sigma_{yt} \geq \sigma_w(t,T) \tag{20}$$

Where,$\sigma_{yt} = Yield\,strength$ and $\sigma_w = working\ strength$,$F_{i,j,k}(t,T)$ thermal force is function of time and 'A' is effective area of aircraft wing structure.

$$\sigma_{yt} \geq \frac{F_{i,j,k}(t,T)}{A} \tag{21}$$

$$F_{i,j,k}(t,T) \geq \sigma_{yt}(t,T)A \tag{22}$$

Failure load of aircraft wing structure can be estimated by Equation 32,

$$F_{i,j,k}(t,T) = \sigma_{yt}(t,T)A \tag{23}$$

5. Solution approach: Runge-Kutta method for simulation of aircraft wing structure

The amplification of round off mistakes that happen in the intermediate stages is a possible issue for the Runge-Kutta method with numerous stages. The important features of RK4 method are as follows:

1] Runge-Kutta method has an error term of order h5 and additionally enables the estimation of the local truncation error at each step in terms of predetermined values.

2] Ralston-Runge-Kuttahas some degree of freedom in assigning the coefficients for a particular Runge-Kutta method. In this approach the values of the coefficients are chosen so as to minimise the truncation error.

3] Butcher-Runge-Kutta method provides higher accuracy at each step, the error being of order h6.

In present study RK4 method is used for structural analysis. The governing equation of second order differential equation for structural analysis of aircraft wing structure is given by Equation 32

$$M\frac{d^2\lambda}{dt^2} + \bar{C}_{ijkl}\lambda = F_{i,j,k}(t,T) \tag{24}$$

Where, C_{ijkl} is fourth order stiffness tensor, F_{ijk}= Thermo mechanical force vector, which is function of time. M=mass matrix of aircraft wing structure. Equation [25] is obtained by rearranging Equation 32

$$\frac{d^2\lambda}{dt^2} + \frac{\bar{C}_{ijkl}}{M} = \frac{F_{i,j,k}(t,T)}{M} \tag{25}$$

Equations [26–28] are obtained by substitute of $\frac{d\lambda}{dt} = \beta$ and $d\lambda = \beta dt$ in Equation 32.

$$\frac{d\beta}{dt} + \frac{\bar{C}_{ijkl}}{M} = \frac{F_{i,j,k}(t,T)}{M} \tag{26}$$

$$F(\beta,t) = \frac{d\beta}{dt} = \frac{F_{i,j,k}(t,T)}{M} - \frac{\bar{C}_{ijkl}}{M} \tag{27}$$

$$\frac{d\lambda}{dt} = \dot{\beta} = F_{i,j,k}(\beta,t) \tag{28}$$

Time dependent force is given for certain time limit, which is transient response of wing structure (refer equations (29-30),

$$F_{i,j,k}(\beta,t) = t^2 + 2t - st\ and\ t = 1 < t < 20 \tag{29}$$

$$F_{i,j,k}(\beta,t) = 1.2S\sin\left(t^2\right) + e^t \text{and time t} = 20 < \text{t} < 40 \tag{30}$$

Boundary condition for length of wing structure: $t = 0$, L = 0 and $t = 20$, L = 100 mm
Boundary condition for width of wing structure: $t = 0$, W = 0 and $t = 40$, W = 100 mm
Where=time, Step size or time interval h= (a-b)/N and a = 0 and b = 20 second, N=number of steps
After solving Equation 32, the solution of fourth order RK4 method is given by Equation 32-Equation 32;

$$t_1 = \beta + \frac{(k_0 + 2k_1 + 2k_2 + k_3)}{6} \tag{31}$$

$$\begin{cases} k_0 = hF_{i,j,k}(\beta, t) \\ k_1 = hf\left(t_i + \frac{h}{2}; \beta + \frac{k_0}{2}\right) \\ k_2 = hf\left(t_i + \frac{h}{2}; \beta + \frac{k_1}{2}\right) \\ k_3 = hf(t_i + h; \beta + k_2) \end{cases} \tag{32}$$

Where, K_0,K_1,K_2 and K_3 are constant of RK4 method it is also function of h(t) and β. The CILAB software Code has been develop for solving transient response of aircraft wing structure. Flowchart describes the detail process for RK4 method (refer Figure 3). The main program is written in SCILAB language to solve the transient response of aircraft wing structure. The approximate solution of differential equations is provided by using the (RK4) method (refer Equation 32-Equation 32). Here initial value of time $t = 0$, N and end value of time. The software finds value of h and proceeds to next step to calculate K0, K_1, $K_2$and K_3.

The cyclic load is applied by specific time interval by using RK4 method. The conversion study has been carrying out for aircraft wing structure subjected to uniform wind pressure (refer Figure 3b). It has been observed that present method is much more accurate as compare to Newton-Raphson method. Deformation of aircraft wing structure is much closer to exact solution method as compare with Newton-Raphson method. Hence RK4 method is most suitable for finding transient response of aircraft wing structure.

6. Numerical results and discussion

In the CAD software, the aircraft wing structure is modelled. A pre-processor is used to characterise boundary conditions and record them in an information document. Clipped edges or symmetry lines are used as boundary conditions. In this research project, simulation is done using the ANSYS software platform and an APDL solver. The software receives input for the necessary material qualities, including elastic, self-healing, and damage criteria. The ductile damage criterion was used.Plastic strains were taken into consideration because bending always occurs with plastic deformation. Here, the major strain and minor strain were both max-principal strains. When an airplane turns, its wing will twist and something will happen. The current work took this effect into consideration. The computational investigation has been carried out based on the static and dynamic failure analysis of aircraft wing structure. The aircraft wing structure is modelled and simulated in ANSYS. For the analysis, the material property of wing structure considered is: Young's Modulus being $E = 2\times10^5$ N/m^{2}and passion ration is 0.25. ANSYS simulation is performed for deformation and stress characteristic of wing structure. The aircraft wing structure model is simulated in Figure 2.

The different stress and deformation values with varying magnitude of wind pressure are tabulated in Table 1. It has been found that when the wind pressure is higher, the stresses and defamation on aircraft wing structures are also higher. On increase in the length of the wing structure from 50 mm to 95 mm, the obtained stress and deformation results are shown in Table 2. Table 3 shows the results on application of external moment to the wing structure. It has been found that as the moment of the wing structure increases, defamation and stress also increases. The obtained results from RK4 method is tabulated in Table 4. Representation in Table 4 shows time dependent displacement

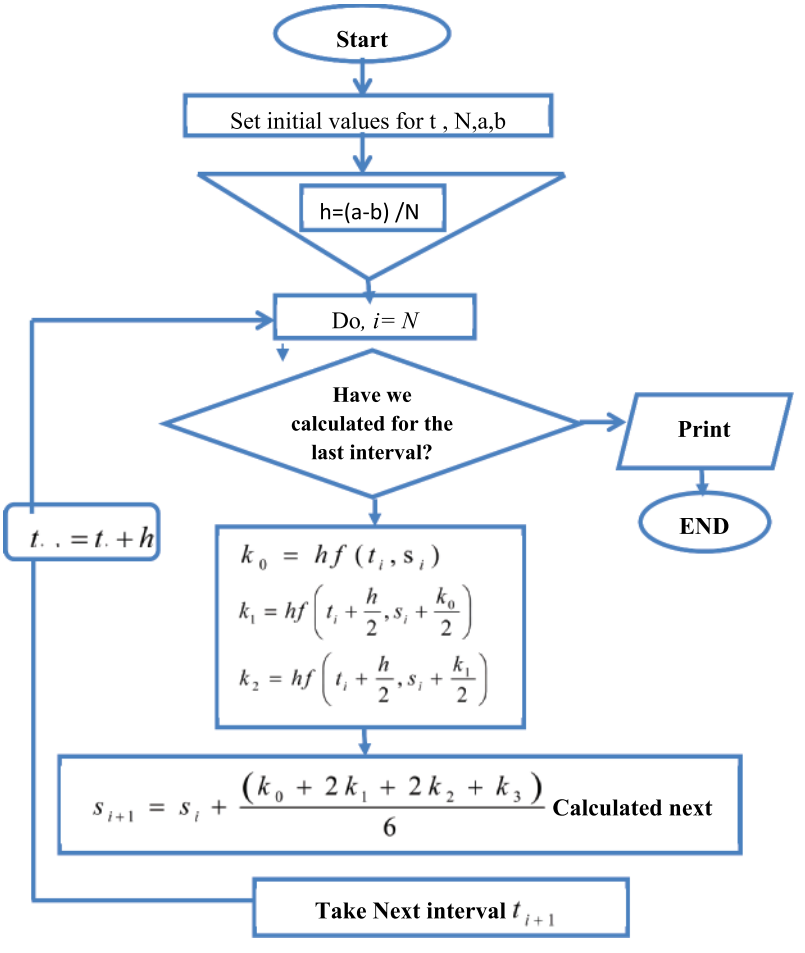

(a)

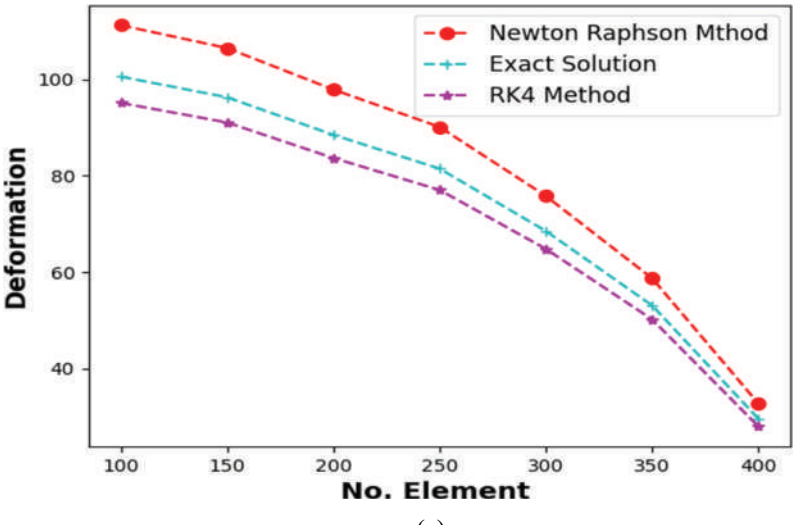

(a)

Figure 3. (a) flowchart of the RK-4 method for resolving the second ODE's systems, (b) the comparison between present (RK4) method with newton-Raphson method and exact solution.

Table 1. Effect of wind pressure on aircraft wing structure.

Wind pressure (MPa)	Deformation (mm)	Stress (σ_1)N/m^2	Stress (σ_3)N/m^2	(τ_{xy})N/m^2
0.5	0.09432	314.84	61.0554	56.434
0.6	0.11319	377.808	73.2664	67.7186
0.7	0.13203	440.776	85.4775	79.0051
0.8	0.1509	503.744	97.6886	90.2915
0.9	0.1697	566.712	109.900	101.578

Table 2. Effect of length of wing on aircraft wing structure.

Length of wing (mm)	Deformation (mm)	Stress (σ_1)N/m^2	Stress (σ_3)N/m^2	(τ_{xy})N/m^2
50	0.0224	176.29	32.0633	63.7289
75	0.06725	277.601	52.142	53.73
85	0.0995	383.5	73.4458	68.559
95	0.14354	505.707	93.404	77.8849

Table 3. Effect of moment on wing structure.

Force moment (N)	Deformation mm	Stress (σ_1)N/m^2	Stress (σ_3)N/m^2	(τ_{xy})N/m^2
12	0.03925	183.535	9.2145	50.627
20	0.06542	305.892	15.3575	84.3789
25	0.081776	382.365	19.19	105.474
30	0.098131	458.838	23.036	126.568
35	0.11448	535.311	26.8757	147.663

Table 4. Numerical results via RK4 method of σ_1 for different wind pressure of aircraft wing structure.

Time (s)	p=50 MPa	p=70 MPa	p=80 MPa	p=100 MPa
1	343.1773	428.9703	514.7633	600.5563
2	381.1863	476.4775	571.7687	667.0599
3	419.201	523.9888	628.7766	733.5644
4	456.4276	570.5119	684.5962	798.6804
5	492.0227	614.9924	737.962	860.9316
6	525.1232	656.3514	787.5795	918.8076
7	554.8807	693.5286	832.1764	970.8243
8	580.4973	725.5268	870.5564	1015.586
9	601.2609	751.4563	901.6517	1051.847
10	616.5779	770.5756	924.5732	1078.571
11	626.002	782.327	938.6521	1094.977
12	629.2551	786.3637	943.4723	1100.581
13	626.2412	782.5662	938.8913	1095.216
14	617.0516	771.0492	925.0469	1079.045
15	601.9596	752.1551	902.3505	1052.546
16	581.4077	726.4372	871.4667	1016.496
17	555.9856	694.6334	833.2813	971.9291
18	526.4022	657.6304	788.8585	920.0867
19	493.4534	616.4231	739.3927	862.3623
20	457.986	572.0703	686.1545	800.2388

response of aircraft wing structure subjected to wing pressure. Dynamics of a simple bar-joint structure is studied for validation purposes. The displacement response of structure in z-direction is shown in Figure 4. It is clear that, the present result trend is very much closed with [14].

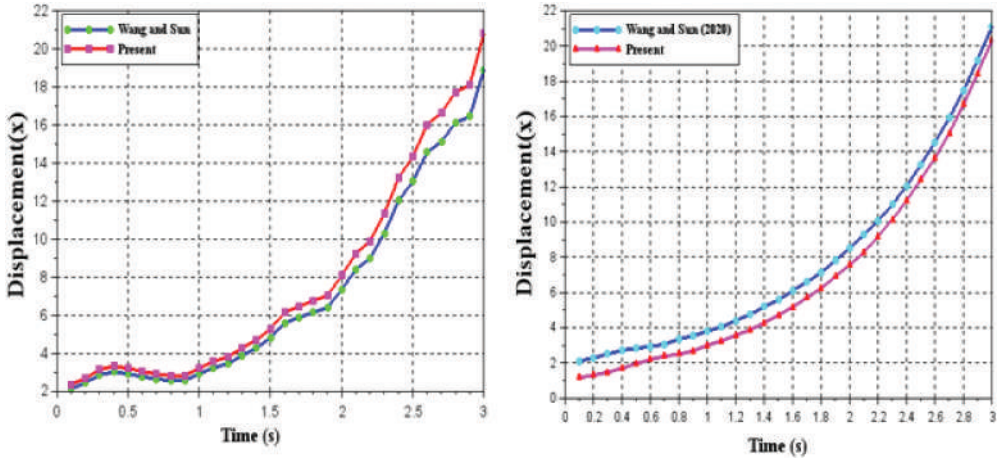

Figure 4. Results compare with [3] displacement along x-direction.

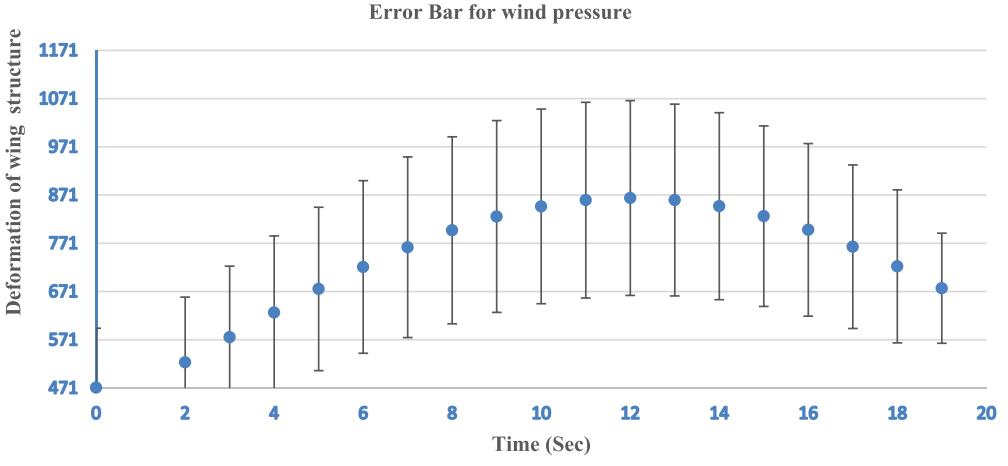

Figure 5. Wind pressure is applied on aerospace wing structure with respective time.

As depicted in Figure 5, the aeronautical wing structure experiences average (Mean) wind pressure. Calculated wind pressure average and standard deviation are presented with corresponding time responses. Error bars, which represent the average and standard deviation of wind pressure, are used to represent how the shape of a wing changes over time. It demonstrates that the error bar can be reduced by using the real value of wind pressure. Since wind pressure fluctuates over time, it is necessary to take into account its average and standard deviation. Figure 6 illustrates how force and moment influence the design of an aircraft wing. It reveals that force increased as deformation increased with regard to time. As the length of the wing structure changed, it was discovered that the deformation value increased over time, as illustrated in Figure 7. In actuality, neither a worker nor a person can accurately set wing length. So, when creating the wing structure,

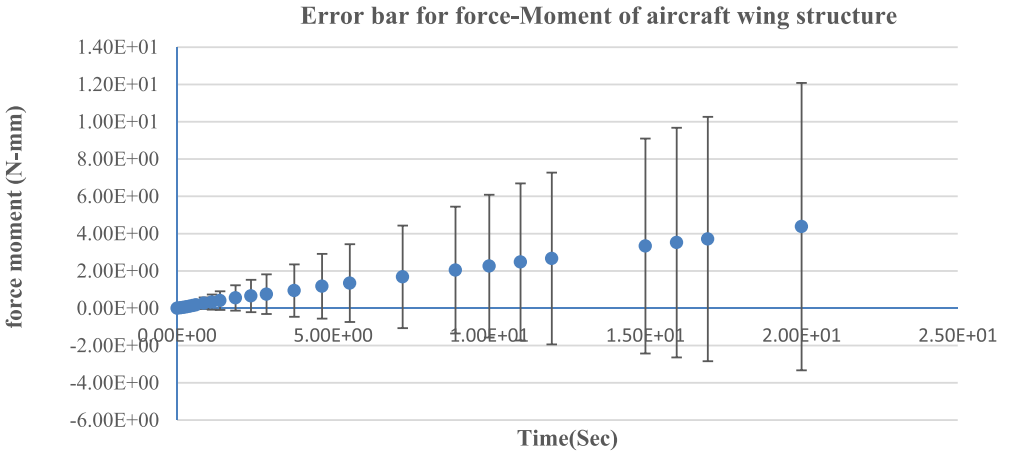

Figure 6. Force-moment is applied on aerospace wing structure with respective time.

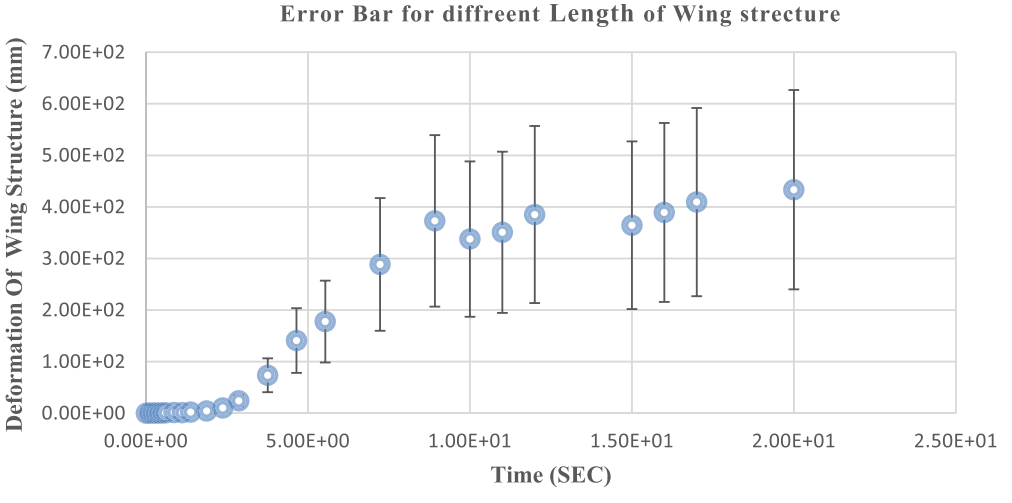

Figure 7. The effect on wing structure subjected to changing in length with different time.

use the mean and standard deviation of length. Figure 7 showed the average and standard deviation (Error Bar) of the length of an aircraft wing structure.

The effect of moment on displacement response of aircraft wing structure is shown in Figure 8(a). It demonstrates that when the force moment and displacement increase, responsiveness also increases with a change in time. However, wind pressure is acted upon wing structure with respect to time is depicted in Figure 8(b). It can be observed that when wind load increase with an increased deformation of aircraft wing structure. The structure of an aircraft wing is shown to bend more when the wind load increases. Figure 9(a) represents deformation versus time for varying Length of wing structure with

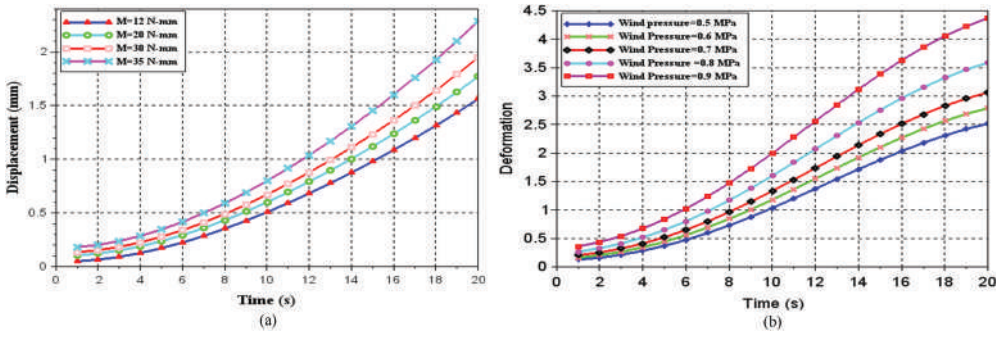

Figure 8. (a) Dynamic response by RK4 method for aircraft wing structure with different moment (b) Deformation time for different wind pressure.

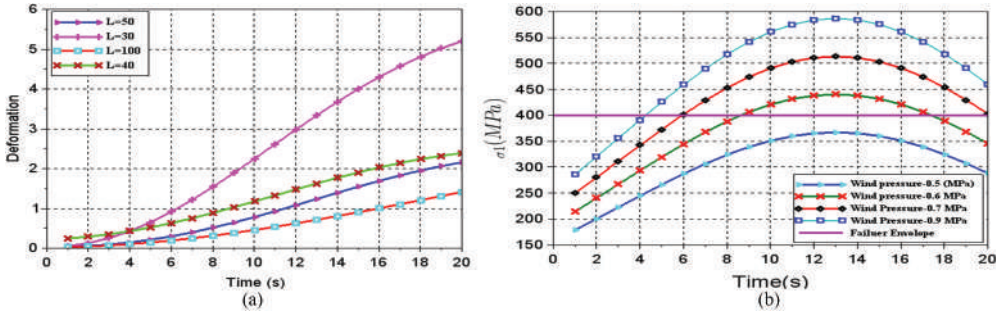

Figure 9. (a) Dynamic response of aircraft wing structure for various length, (b) principle stress vs time is executed by RK4 method for dynamic failure envelope.

uniform wind pressure. It is observed that when L = 30 mm, then the deformation is large since length is shorter. Figure 9(b) shows the dynamic failure of wing structure for different wind pressure. It demonstrates that when a wind pressure of 0.5 MPa is applied to an aircraft's structure, no failure occurs within 20 seconds, but when the wind pressure is increased to 0.6 or 0.9, failures do occur within the same time frame of 20 seconds. The principle (∂) with respect to time for different length of wing structure is plotted in Figure 10(a). It has been observed that structures with lengths of 50 and 100 mm do not experience failure envelopes, while failure occurs with lengths of 30 and 40 mm. Similarly, Figure 10(b) is represents dynamic failure envelope for different moment of aircraft wing structure. It demonstrates that when a moment is applied to a wing structure up to 25 N-mm, failure doesn't happen for 20 seconds, but when a moment of 30 N-mm or more is applied, failure happens from 6 seconds and above. Failure stress for different pressure is shown in Figure 11(a). It has been noted that when wind pressure is above 0.9 MPa, a structure fails. The impact of the L/b ratio on the failure of the aircraft wing structure, as depicted in Figure 11(b), is also examined. It is evident that when the L/b ratio is 40, the structure does not fail since the wind structure is more robust than other ratios.

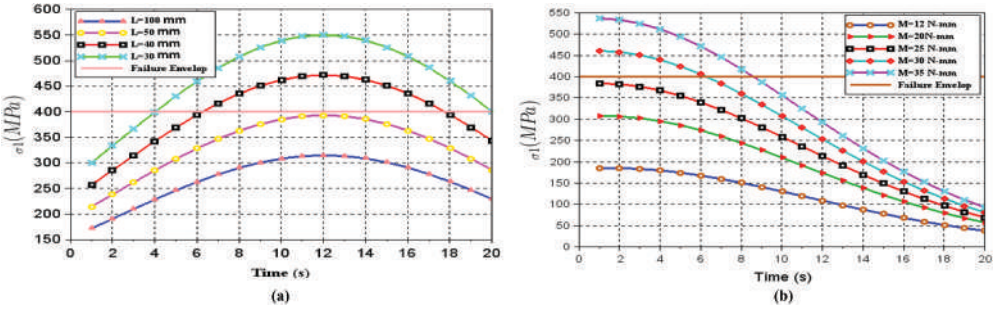

Figure 10. (a) Dynamic failure envelope for different length of aircraft wing structure,(b) dynamic failure envelope for different moment of aircraft wing structure.

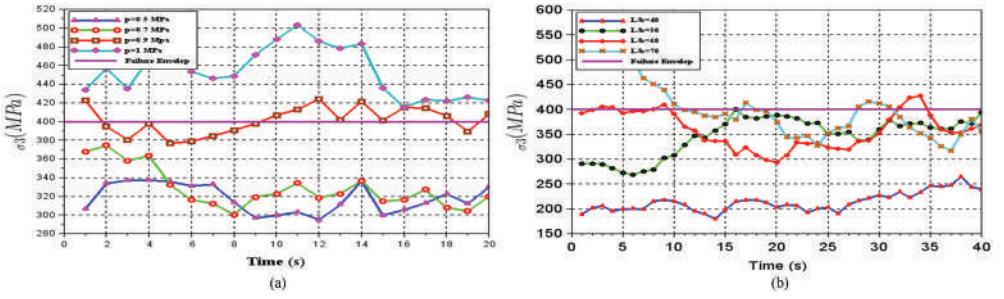

Figure 11. (a) Dynamic failure envelope for different wind pressure of aircraft wing structure, (b) principle stress v/s time of failure criteria for different L/b ratio.

7. Conclusion

In this article, a methodology for predicting aircraft wing structural failure and the impacts of self-healing on mechanical properties of structures has been developed. The RK4 numerical approach has been effectively used in aerospace and aeronautical applications. The proposed work is mainly focused on the failure effect of an aircraft's structure.The major conclusions can be summarised as follows:

(1) A RK4 computational method is developed to compute dynamics failure analysis of aircraft wing structures.
(2) The current work is concerned with the impact of moment, wind pressure, and L/B ratio on dynamic reactions such displacement and stress of wing components during motion. Failure stress criteria are also discussed.
(3) The proposed RK4 approach is verified using the framework of existing literature, and a mathematical model for aircraft wing structure is developed and incorporated into the SCILAB code.
(4) The work may be useful for the designers of the aerospace structures. The outcomes of the current research work may also be useful for design and manufacturing in the automobile sector.

Disclosure statement

No potential conflict of interest was reported by the author(s).

ORCID

Ankit D. Oza http://orcid.org/0000-0001-8104-1266

References

[1] Abderezak R, Hassaine T, Rabia B. New solution for damaged porous RC cantilever beams strengthening by composite plate. Adv Mater Sci Eng. 2021;10(3):169–194. doi: 10.12989/amr.2021.10.3.169

[2] Ali B, Omar W. Similarity solution and RungeKutta method to a thermal boundary layer model at the entrance region of a circular tube: the Leveque approximation. Revista Científica. (31): 6–18. doi: 10.14483/23448350.12506

[3] Broatch MC, García-Tíscar J, García-Tíscar J. Spectral analysis and modelling of the spray liquid injection in a Lean Direct Injection (LDI) gas turbine combustor through Eulerian-Lagrangian large Eddy Simulations. Aerospace Science And Technology. 2021;118:106992. doi: 10.1016/j.ast.2021.106992

[4] Du X, Jin L, Ma G. Numerical simulation of dynamic tensile-failure of concrete at meso-scale. Int J Impact Eng. 2014;66:5–17. doi: 10.1016/j.ijimpeng.2013.12.005

[5] Fang J, Jiang ZD, Qi J, et al. Dynamic failure analysis of bimaterial beam with crack tip terminating interface. AdhesivesEngineering. 1993;1999:229–237.

[6] Jiang X, Qian Y, Zhang J, et al. Research on seismic dynamic response characteristics of weak surrounding rock slope with double-arch tunnel, research square. https://orcid.org/0000-0003-0003-916X .

[7] Kim D, Lee Y, et al. Aerodynamic analysis and static stability analysis of manned/unmanned distributed propulsion aircrafts using actuator methods. J Wind Eng Ind Aerodyn. 2021;214:214 104648. doi: 10.1016/j.jweia.2021.104648

[8] Lai T, Ting-Hua Y, Li H, et al. An explicit fourth-order Runge–Kutta Method for dynamic force identification. Int J Str Stab Dyn. 2017;17(10):1750120–1750121. doi: 10.1142/S0219455417501206

[9] Qiu Z, Zhu B. A Newton iteration-based interval analysis method for nonlinear structural systems with uncertain-but-bounded parameters. Int J Numer Methods Eng. 1–22. doi: 10.1002/nme.6751.

[10] Rahi MJ, Firoozjaee AR. Simplified numerical method for nonlocal static and dynamic analysis of a graphene nanoplate. Adv Mater Sci Eng. 10(1):1–22. doi: 10.12989/amr.2021.10.1.001.

[11] Rizov V. Analysis of the strain energy release rate for time-dependent delamination in multilayered beams with creep. Adv Mater Sci Eng. 11(1):41–57. doi: 10.12989/amr.2022.11.1.041.

[12] Said S, Tanougast C, Azzaz M, et al. Design and FPGA implementation of a wireless hyperchaotic communication System for secure real-time image transmission. Eurasip J Image Video Process. 2013;43.

[13] Shuai H, Lv Y, Peng Y, et al. Effect of different groundwater levels on seismic dynamic response and failure mode of Sandy Slope. Plos One. 2015;11:1–11.

[14] Wang Y, Sun B.A. Computational method for dynamic analysis of Deployable structures. Shock Vib. 10. doi: 10.1155/2020/2971784.

[15] Xing-Yu W, Li-Shuai J, Xing-Gang XU, et al. Numerical analysis of deformation and failure characteristics of deep roadway surrounding rock under static-dynamic coupling stress. J Cent South Univ. 28(2):543–555. doi: 10.1007/s11771-021-4620-2.

[16] Xinrong L, Yongquan L, Lu Y, et al. Numerical analysis of evaluation methods and influencing factors for dynamic stability of bedding rock slope. J Vibroeng. 2017;19 (3):1937–1961. doi: 10.21595/jve.2016.17210
[17] Zhou Z, Ren C, Xu G, et al. Dynamic failure mode and dynamic response of high slope using shaking table test. Shock Vib. 19. doi: 10.1155/2019/4802740.
[18] Usefvand M, Maleki A. Cyclic behavior and performance of a coupled-steel plate shear wall with fuse pin. Adv Mater Sci Eng. 10(3):245–265. doi: 10.12989/amr.2021.10.3.245.
[19] Ahmed RA, Raad M, Fenjan LBH, et al. A review of effects of partial dynamic loading on dynamic response of nonlocal functionally graded material beams. Adv Mater Sci Eng. 9 (1):33–48. doi: 10.12989/amr.2020.9.1.033.
[20] Basyir A, Bura RO, Lesmana D, et al. Evaluation of steel and tungsten carbide – cobalt (WC-8Co) 5.56 × 45 mm calibre projectile penetration into Silicon carbide (SiC): experiment and numerical simulation. Def Sci J. 2022 March;72(2):205–216. doi: 10.14429/dsj.72.17232
[21] Bhadra MK, Gopalan V. Stress redistribution near a crack in Maraging steel using composite patch. Def Sci J. 2021 November;71(6):816–821. doi: 10.14429/dsj.71.16794
[22] Singh S, Khan DC. Tip radius effect on fatigue crack growth and near - tip fields in plastically compressible materials. Def Sci J. 2021 March;71(2):248–255. doi: 10.14429/dsj.71.15983.
[23] Chibani S, Coudert F-X. Machine learning approaches for the prediction of materials properties. APL Mater. 2020;8:080701. doi: 10.1063/5.0018384
[24] Patel G, Ganesh MK, Kulkarni O. Experimental and numerical investigations on forming limit curves in micro forming. Adv Mater Process Tech. doi: 10.1080/2374068X.2020.17932
[25] De Nardi C, Bullo S, Cecchi A, et al. Self-healing capacity of advanced lime mortars. Advances In Materials And Processing Technologies. 2016;2(3):349–360. doi: 10.1080/2374068X.2016.1191896
[26] Zhao L, Ren Z, Liu X, et al. A multifunctional, self-healing, self-adhesive, and ConductiveSodium Alginate/Poly(vinyl alcohol) composite hydrogel as aFlexible strain sensor. ACS Appl Mater Interfaces. 2021;13:11344–11355. doi: 10.1021/acsami.1c01343
[27] Kasambe PV, Bhole KS, Bhoir DV. Analytical modelling, design optimisation and numerical simulation of a variable width cantilever beam MEMS switch, Taylor and Francis. Adv Mater Process Technol. 2021;8(3):2850–2870. doi: 10.1080/2374068X.2021.1945263
[28] Kasambe PV, Bhole KS, Bage AA, et al. Analytical modeling and numerical investigation of a variable width piezoresistive multilayer polymer micro-cantilever air flow sensor. Adv Mater Process Technol. 2022;8:4365–4383. doi: 10.1080/2374068X.2022.207697410.1080/2374068X.2022.2076974
[29] Farooqui TA, Belwanshi V, Rane K, et al. Numerical analysis of Joule heating in a Ni–Ti segmented wire used in sensing applications. J Inst Eng India Ser. 2022;D:301–308. doi: 10.1007/s40033-022-00392-4